

Solid-State Absorption Spectroscopy and Spectroscopic Observation of a Laser-Induced Metastable State in Dibromobis-(4-methylthiazole)nickel(II)

Loïc Le Guilly, Nathalie Desmangles and Christian Reber*

Contribution from the Département de chimie, Université de Montréal, Montréal, Québec, Canada H3C 3J7

Received: January 25, 1995

Accepted (in revised form): March 1, 1995

Résumé

La spectroscopie d'absorption à l'état solide dans la région du visible et du proche-infrarouge est utilisée pour caractériser le dibromobis(4-méthylthiazole)nickel(II), un composé qui montre une transition thermochromique irréversible. Le spectre d'absorption est composé de trois bandes intenses à 4,000-6,000 cm^{-1} , 8,900 cm^{-1} et 15,200 cm^{-1} qui correspondent aux transitions permises par le spin. Leurs énergies et intensités indiquent une géométrie de coordination tétraédrique pour le chromophore de la forme bleue du composé. La géométrie tétraédrique déformée est confirmée par les bandes faibles et étroites observées entre 20,000 cm^{-1} et 26,000 cm^{-1} , attribuées aux transitions interdites par le spin. Le contrôle de la transition thermochromique par excitation laser nous a permis d'isoler le composé dans un état métastable. Cette approche est plus rapide que le changement de forme par traitement thermique. La durée de vie de l'état métastable du dibromobis(4-méthylthiazole)nickel(II) est de plus d'une heure à 30 K, de 20 min à 80 K et de moins de 5 min à 150 K, indiquant une relaxation thermique de l'état métastable.

Abstract

Solid-state absorption spectroscopy in the visible and near-infrared spectral regions is applied to dibromobis(4-methylthiazole)nickel(II), a compound reported to be irreversibly thermochromic. Three intense spin-allowed transitions are observed at 4,000-6,000 cm^{-1} , 8,900 cm^{-1} and 15,200 cm^{-1} . Their energies and intensities are indicative of a tetrahedral coordination geometry of nickel(II) in the blue single-crystal-line form of the compound. The sharp, polarized spin-forbidden transitions observed between 20,000 cm^{-1} and 26,000 cm^{-1} confirm a distorted tetrahedral coordina-

tion geometry. Laser excitation into an excited electronic state leads to a partial inversion of the thermally irreversible thermochromism, trapping the title compound in a metastable state. Optical switching between the two forms of this thermochromic system is much faster than the traditional thermal switching. The laser-induced metastable state of dibromobis(4-methylthiazole)nickel(II) has a lifetime of more than 1 h at 30 K, 20 min at 80 K and less than 5 min at 150 K, indicative of thermal relaxation.

Keywords: VIS/NIR absorption spectroscopy, thermochromism, optical switching, crystal field calculations, tetrahedral nickel(II) complexes

Introduction

Absorption spectroscopy is a very powerful method to elucidate the electronic structure of materials containing transition metal ions. Excited-state energies, symmetries and structural distortions all can be obtained from the optical spectra of transition metal compounds (1-5). In the recent literature, absorption spectroscopy has been extensively used to develop a detailed picture of the spin-crossover phenomena in iron(II) compounds, phase transitions that are often accompanied by dramatic color changes. The dynamics of these transitions have been investigated with a variety of optical spectroscopic methods, and it has been shown that irradiation with laser light at wavelengths where the absorbances of the high-spin and low-spin forms are different can be used to rapidly switch between the two forms of these compounds (6,7). Optical and thermal switching are two different approaches to the control of the spin-crossover transitions and therefore the color of these materials. A more general category of transition metal complexes that show phase transitions

accompanied by color changes are thermochromic compounds, described and reviewed extensively in the literature (8).

A particularly interesting thermochromic compound showing a blue and a yellow form is dibromobis(4-methylthiazole)nickel(II). This system is reported to be irreversibly thermochromic because the yellow form of the compound is converted to the blue form at room temperature within minutes, but the transition from the blue to the yellow form can not be observed at any temperature (8,10). Several different blue forms of the title compounds were reported, indicating the importance of controlled synthesis and crystallization conditions (9,10). Our procedures are described in the following section. We consistently obtained good quality single crystals and amorphous deposits from absolute methanol solutions under nitrogen. The blue form of the title compound and the analogous compound of cobalt(II) are reported to be isomorphous (10). Diffuse reflectance spectra at room temperature are reported for both the blue and yellow forms and are in good agreement with our solution and solid-state spectra (9,10).

The goals of our work are twofold. First, detailed absorption spectra of the title compound in both the visible and near-infrared (NIR) spectral regions are used to determine the type of coordination geometry of the nickel(II) centers in the blue form of the compound. Both octahedral and tetrahedral coordinations were proposed in the literature (9,10). Our spectroscopic results further show that there exist at least two well-defined modifications of the blue form in the solid state, resolving another controversy in the literature (9,10). Second, we use laser irradiation to trap the blue compound in a long-lived metastable state, most likely the yellow form, analogous to the behavior of iron(II) spin-crossover systems. The low-temperature optical experiments with the sample in a helium atmosphere prevent possible thermal decomposition and exclude any influence of the ambient atmosphere on the sample, factors that are very likely to influence the thermochromic behavior of the title compound. Optical switching offers therefore an alternative route to reversible transitions between different forms of thermochromic compounds, an essential prerequisite for potential applications.

Experimental

The title compound was synthesized using literature methods (9-11). The purities of 4-methylthiazole and the blue form of the title compound were checked by comparing their infrared spectra with literature data (10). Dark blue, rectangular single crystals were obtained by slow evaporation of absolute methanol solutions at room

temperature under nitrogen over several days. These crystals are air-stable and show easily discernible extinction directions between crossed polarizers, allowing us to measure the polarized absorption spectra described in the following section. Solid deposits on round quartz plates with a diameter of 10 mm were obtained within several hours from concentrated solutions of the title compound in methanol, again under nitrogen. The thickness of these slightly hygroscopic solid deposits varied between 60 μm and 300 μm , and they were of a lighter blue color than the single crystals. No crystals were obtained by evaporation of solutions not under an inert atmosphere. The resulting light-blue powders were very inhomogeneous when inspected under a microscope and decomposed to gray products over several days, confirming literature reports that indicate the title compound to be hygroscopic (9). These solids were not used for spectroscopic measurements. The yellow form of the compound was obtained from ethanol solutions, and showed a thermochromic transition to the blue form as reported in the literature (10). No crystals or high-purity solid deposits of the yellow compound could be obtained because of its rapid conversion to the blue form, preventing us from making detailed solid-state spectroscopic measurements.

All the absorption spectra were measured with a Varian Cary 5E spectrometer equipped with a pair of Glan-Taylor polarizers. The samples were mounted in a helium gas-flow cryostat (Oxford Instruments CF-1204). Typical dimensions of the solid samples were approximately 1 mm x 1 mm. The samples were mounted on black anodized aluminum plates with holes drilled to match the size and shape of the sample. A helium-neon laser (Melles Griot LHR 141, 10 mW) was used for sample irradiation. For these experiments, it was of crucial importance to leave the position of the sample and the cryostat in the spectrometer unchanged. In order to guide the laser beam, we added a mirror at an angle of 45° to the optical path of the spectrometer for irradiation of the sample. The direction of the laser beam was therefore parallel to the sample beam of the spectrometer and was adjusted to pass exactly through the hole in the aluminum plate holding the sample. With this experimental setup we could irradiate exactly the same regions of the solid sample that were used for the absorption measurements. Irradiation times varying from a few minutes to an hour were used, but no effects specific to the duration of the irradiation were observed. Absorption spectra at specific times after irradiation were measured at a scan speed of 1200 nm/min, leading to acquisition times of less than one minute per spectrum, a time resolution sufficient for the relaxation kinetics described in the second section of the discussion.

Spectroscopic Results

Solution absorption spectra of the two forms of the title compounds are presented in Figure 1 and illustrate the very distinct spectroscopic properties of each form. The band positions for the blue form in the visible spectral region are very similar to those obtained from diffuse reflectance spectra in ref. (10) and to the solid-state spectra reported in the following. The diffuse reflectance spectrum of the blue form of the title compound in ref. (9) shows bands at $22,500\text{ cm}^{-1}$ and $23,000\text{ cm}^{-1}$ that are not observed in ref. (10) and in our experiments, and are most likely due to a different chromophore. The yellow form of the title compound shows no clearly resolved bands in the visible range, its spectrum is dominated by the onset of a strong band in the ultraviolet. A weak shoulder is observed at $19,000\text{ cm}^{-1}$, corresponding to one of the two bands in the diffuse reflectance spectrum of the yellow form (10). The other band in the spectral region of Figure 1 is at $22,100\text{ cm}^{-1}$, (10) and we observe a weak shoulder at $25,500\text{ cm}^{-1}$. The agreement with literature data is satisfactory for both forms, especially in view of the differences between diffuse reflectance and solution spectra.

The absorption spectra of the blue crystalline form of the title compound reveal much more detail than the solution spectra and are shown in Figure 2 for the visible and near-infrared spectral regions. All the high-quality single crystals had absorbances at the wavelengths of the most intense band maxima that are outside the range of our spectrometer, the spectra are therefore cut off at absorbances of 3.4 and 1.4 in the visible and near-infrared, respectively. The most important spectroscopic features are nevertheless easily recogniz-

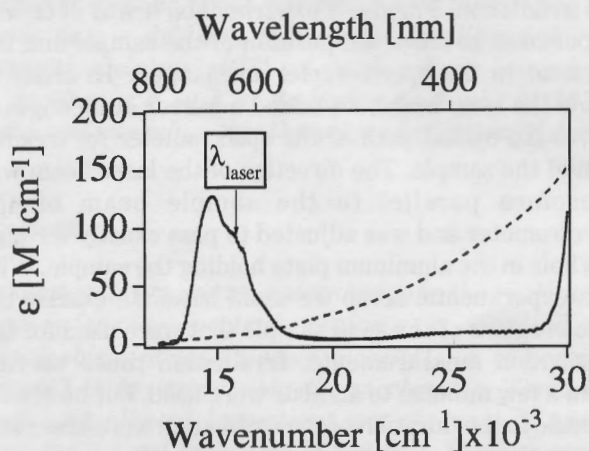


Figure 1. Absorption spectra of the blue and yellow forms of the title compound in solution. The solid and dotted lines denote the spectrum of the blue and yellow forms in acetone and ethanol, respectively. The laser wavelength used for the optical switching from the blue to the yellow form is indicated by an arrow.

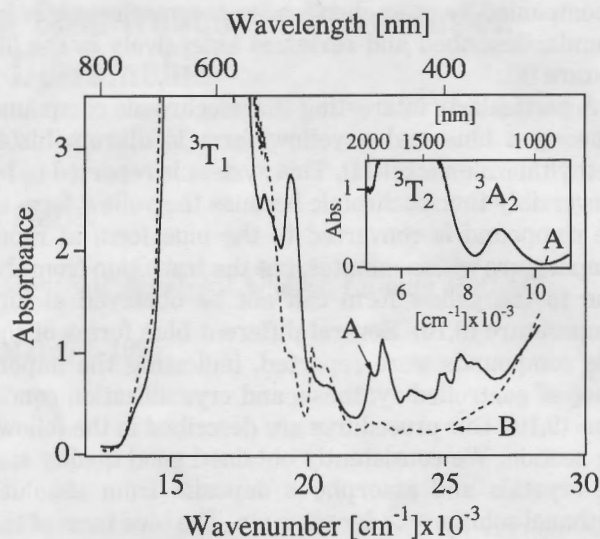


Figure 2. Polarized single-crystal absorption spectra of dibromobis(4-methylthiazole)nickel(II) at 80 K. Solid and dotted lines denote polarized spectra of the crystal. Polarizations A and B are along the extinction directions of the crystal. The inset shows the near-infrared absorption spectrum in polarization A only. Note the different absorbance scales for the main Figure and the inset. The final electronic states of the spin-allowed transitions are indicated at the band maxima in the Figure.

Table I. Observed and calculated transition energies for dibromobis(4-methylthiazole)nickel(II). Parameter values for the crystal field calculation are $10 Dq = 4,850\text{ cm}^{-1}$, $Ds = 400\text{ cm}^{-1}$, $Dt = 40\text{ cm}^{-1}$, $B = 920\text{ cm}^{-1}$, $C = 4,330\text{ cm}^{-1}$

Observed Energy [cm^{-1}]	Assignment (T_d symmetry)	Polarization, ^a Intensity ^b	Calculated Energy [cm^{-1}]	Electronic State (T_d , D_{2d} point groups)
			0	$3T_1, 3A_2$
			600	$3T_1, 3E$
4,000	$3T_1 \rightarrow 3T_2$	A, s	4,090	$3T_2, 3B_2$
6,700	$3T_1 \rightarrow 3T_2$	B, s	4,420	$3T_2, 3E$
8,900	$3T_1 \rightarrow 3A_2$	B, s	8,940	$3A_2, 3B_1$
15,200	$3T_1 \rightarrow 1T_2, 1E$	A, B, sh	14,250	$1T_2, 1B_1$
			14,970	$1E, 1B_1$
			15,080	$1T_2, 1E$
			16,180	$1E, 1A_1$
16,000	$3T_1 \rightarrow 3T_1$	A, B, s	16,800	$3T_1, 3E$
			18,730	$3T_1, 3A_2$
19,400		B, w		
20,150		A, w		
20,600		A, w		
22,300		B, w	21,850	$1T_2, 1B_2$
22,700		B, w	22,000	$1T_2, 1E$
23,500		B, w		
23,700		B, w	23,620	$1T_1, 1E$
23,900		B, w	24,040	$1A_1, 1A_1$
24,800		B, w		
25,000		B, w		
25,500		B, w	25,600	$1T_1, 1A_2$
25,600		B, w	25,980	$1E, 1A_1$
25,950		B, w		
26,150		B, w	26,980	$1E, 1B_1$
			54,970	$1A_1, 1A_1$

^a polarizations A, B as indicated in Figures 2, 3. ^bs: strong, sh: shoulder, w: weak

able. We notice three broad, intense bands centered at approximately 1600 nm, 1120 nm and 600 nm. Less intense, sharp bands were observed in the visible between 570 nm and 390 nm. They have distinct polarizations, indicative of the high quality of the crystals, as illustrated in Figure 2. Observed transition energies are summarized on the left hand side of Table I.

The comparison between spectra of single crystals and solid deposits reveals some characteristic similarities and differences. The overall spectra in the visible spectral region are compared in Figure 3a and show similar general features. Both spectra are dominated by a broad band centered at approximately 600 nm and show weaker bands at shorter wavelengths. A closer examination reveals important differences between the

spectra. The intense visible absorption band in the solid deposit has its maximum at lower energy than the dark blue crystalline form. The spectrum of a very thin single crystal is included in Figure 3a and clearly illustrates the different bandshape and band maxima for the two different solids. The resolved structure observed on the intense absorption band is also different for the two blue modifications of the title compound. No polarization effects were observed for the solid deposit, indicating its amorphous nature and possibly inferior quality of the surfaces. The energy separation of the resolved maxima on the intense absorption band of the deposit, between $13,000\text{ cm}^{-1}$ and $17,000\text{ cm}^{-1}$ in Figure 3a, is not constant, it varies from 520 cm^{-1} to 730 cm^{-1} and does therefore not correspond to a simple vibronic progression. The structure is most likely due to both vibronic effects and multiple electronic states, in analogy to the spectrum of K_2NiO_2 , where similar irregular vibronic structure was quantitatively analyzed(12). The crystal field model presented in the first part of the discussion in fact confirms the presence of multiple electronic states in this region of the spectrum. Figure 3b shows details of the sharp bands in the spectra of both single crystals and deposits. Again, the spectrum of the deposit shows no polarization effects and the energies of the weak, sharp bands are clearly different from those observed for the single crystals. The widths of these absorption bands in the deposit are on the order of 300 cm^{-1} , larger by a factor of five than the widths of the sharpest bands in the single crystals. These relatively narrow widths and the excellent reproducibility of the spectra nevertheless indicate a relatively ordered structure for the solid deposit.

The spectroscopic evidence for a metastable form of the solid deposit is summarized in Figure 4. The difference spectra at 80 K in the main Figure were obtained by subtracting the spectrum measured at a certain time after the laser irradiation from a reference spectrum measured immediately before laser irradiation. The difference traces show an obvious trend in the region of the intense absorption band in the visible region, framed by the two vertical lines in Figure 4. At short times after irradiation we observe a positive difference, indicating that the intense absorption band has become weaker by approximately 5% after irradiation. At long times, this difference vanishes, as illustrated by the traces measured 35 min and 60 min after irradiation. A negative difference is obtained between $20,000\text{ cm}^{-1}$ and $25,000\text{ cm}^{-1}$ at short times, indicative of increasing absorption intensity in the green-blue region for the metastable intermediate formed at 80 K after laser irradiation. This observation provides qualitative evidence for the formation of the yellow modification of the title compound. The negative and positive differences are

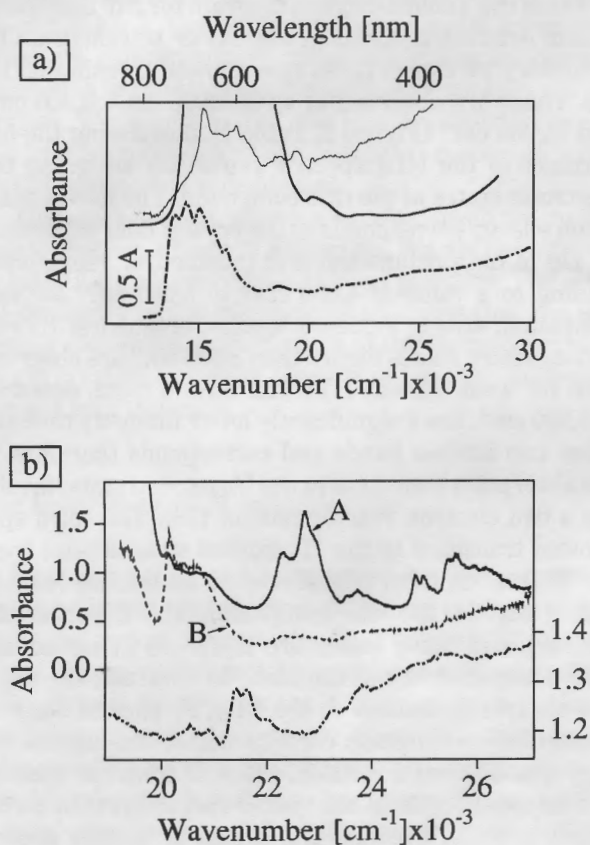


Figure 3. Comparison of absorption spectra of single crystals and solid deposits of dibromobis(4-methylthiazole)nickel(II). (a) Unpolarized visible absorption spectra of the same single crystal as in Figure 2 (solid line), a thin single crystal (thin solid line) and a solid deposit (dot-dashed line, bottom trace) at 300 K. The absorbance scale applies to the spectrum of the solid deposit only. (b) Enlarged view of the resolved structure in the polarized single-crystal spectra shown in Figure 2 (solid and dotted lines, left-hand ordinate scale, polarizations as in Figure 2) and resolved structure in the spectrum of the solid deposit at 80 K (dot-dashed line, right-hand ordinate scale).

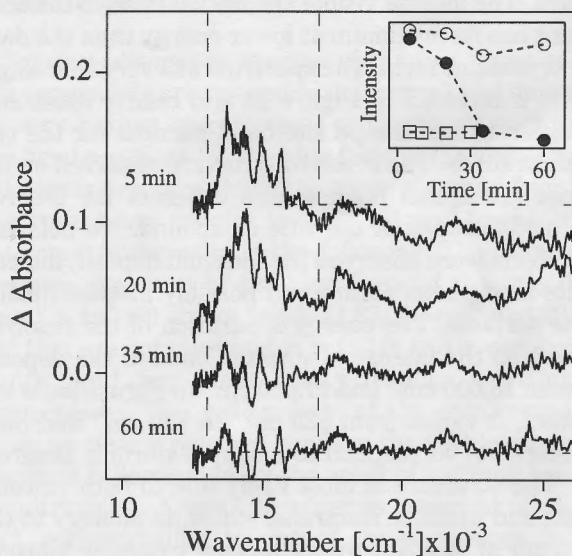


Figure 4. Changes in the absorption spectrum after laser irradiation of a solid deposit of dibromobis(4-methylthiazole)nickel(II) at 632.8 nm. The traces shown in the main figure were determined from spectra measured at 80 K and are offset for clarity by 0.05 absorbance units. The ordinate labels apply to the trace obtained 35 minutes after laser irradiation. Horizontal baselines are given for the traces obtained 5 min and 60 min after irradiation as guides for the eye. The inset shows the integrated absorption intensity between 13,000 cm^{-1} and 17,000 cm^{-1} denoted by the dashed vertical lines in the main Figure, as a function of time at 30 K (open circles), 80 K (full circles) and 150 K (open squares).

clearly seen by comparing the spectra measured 5 min and 60 min after irradiation with the horizontal baselines included in the Figure. The traces obtained 35 min and 60 min after irradiation are very similar, indicative of the accuracy of our spectroscopic instrumentation for the determination of difference spectra. The inset to Figure 4 shows integrated intensities of the difference spectra in the region indicated by the vertical lines at three temperatures. The most important changes of integrated absorption intensity with time are observed at 80 K. At 30 K, a large and almost constant positive difference is observed, and the difference at 150 K is negligible even at the shortest times after irradiation. These observations will be analyzed in the second section of the discussion. We exclude laser heating effects to cause these time-dependent differences, because of the very low power of our laser, and also because such heating effects are not expected to persist over long times after irradiation.

Discussion

The coordination geometry of Ni^{2+} in dibromobis-4-methylthiazolenickel(II)

The detailed absorption spectra obtained from single crystals of the title compound allow us to determine the type of coordination geometry of the nickel(II) centers. Magnetic measurements in the literature report a ground state moment of 3.36 B.M., on the borderline between typical values for nickel(II) in tetrahedral and octahedral coordination (13). In this section, we present an assignment of the spectroscopic transitions leading to the conclusion that the title compound has a distorted tetrahedral coordination geometry.

From the Tanabe-Sugano diagram for a d^8 configuration in octahedral (point group O_h) or tetrahedral (T_d) symmetry we expect three spin-allowed transitions (14-16). These are observed at 4,000-6,000 cm^{-1} , 8,900 cm^{-1} and 15,200 cm^{-1} (Figure 2, Table I), illustrating the importance of the NIR spectral region for assigning the electronic states of the title compound. The lowest transition energy corresponds to the crystal field parameter 10 Dq in both octahedral and tetrahedral geometries, leading to a value of 4,000 cm^{-1} to 6,000 cm^{-1} for this compound, strong evidence against octahedral coordination, where values higher than 8,000 cm^{-1} are observed even for weak ligands (17). The second band, centered at 8,900 cm^{-1} , has a significantly lower intensity than the other two intense bands and corresponds therefore to the absorption transition to the 3A_2 excited state, involving a two electron rearrangement (18). The third spin allowed transition to the 3T_1 excited state arising from the 3P free ion term is observed as an intense band at 15,200 cm^{-1} in the title compound. The experimental intensities of these bands are therefore in agreement with a tetrahedral coordination. In contrast, the weak two-electron transition to the $^3T_{1g}(^3F)$ excited state in octahedral coordination corresponds to the highest energy spin-allowed transition, different from our spectra.

The weak bands in the visible spectral region correspond to spin-forbidden transitions to singlet excited states. Many of these states arise from the same strong-field configuration as the ground state, giving rise to the sharp bands shown in Figure 3b. Their assignment is not straightforward, but the clear polarization observed in the experimental spectra indicates significant deviations from perfect tetrahedral symmetry, for which unpolarized bands are expected.

In order to quantitatively interpret the spectra, we compared crystal field calculations for a d^8 ion in tetrahedral coordination to the experimental data. We first adjusted the band positions of the spin-allowed

transitions by varying the parameters 10 Dq and B, leading to values of 4,850 cm⁻¹ and 920 cm⁻¹, respectively. The latter value corresponds to 88% of the Racah parameter B for the free Ni²⁺ ion (15). The ratio of C/B was kept constant at 4.71 (15). The tetrahedral model reproduces the observed maxima of the spin allowed transitions reasonably well, but both the number and energies of the spin-forbidden transitions are unsatisfactory. We therefore lowered the point group symmetry in our model from T_d to D_{2d}, allowing nonzero values for the crystal field parameters Ds and Dt (14). All the calculated levels obtained with this model are listed in Table I. The crystal field parameters Ds and Dt are smaller by an order of magnitude than 10 Dq, the tetrahedral splitting. The number and energies of the weak spin-forbidden transitions obtained in D_{2d} symmetry agree much better with the experimental data in Figure 3b and Table I. The number of bands is still lower than observed experimentally, most likely due to vibronic sidebands or multiple inequivalent chromophores in the crystal. We conclude that the blue crystalline form of the title compound contains nickel(II) centers in a distorted tetrahedral coordination.

The solid deposit shows a similar spectrum to the single crystals, shown in Figure 3a. We did not attempt to quantitatively reproduce its band positions. The overall similarity of the two spectra indicates that the molecular coordination geometries of the chromophores in single crystals and solid deposits of the title compound are not very different.

The Laser-induced Metastable State

The title compound is reported to be irreversibly thermochromic, and thermal switching is possible only from the yellow form to the blue form (8,10). In this work, we use optical switching by laser excitation of the solid deposit to reverse the transition by a pathway involving an excited electronic state. The approach is schematically illustrated in Figure 5. The blue form of the solid deposit is stable at low temperature and efficiently absorbs laser light with a wavelength of 632.8 nm, indicated by the solid arrow in Figure 5. The absorbance of the blue form at this wavelength is higher by at least an order of magnitude than the absorbance of the yellow form, as illustrated by the solution absorption spectra in Figure 1, where the extinction coefficient of the blue form is higher by a factor of 12 at the laser wavelength. Relaxation from the excited state populated by the laser excitation occurs into both low-energy states corresponding to the two forms of the title compound. These relaxation processes are indicated by the dashed arrows in Figure 5. At low temperatures, we expect to

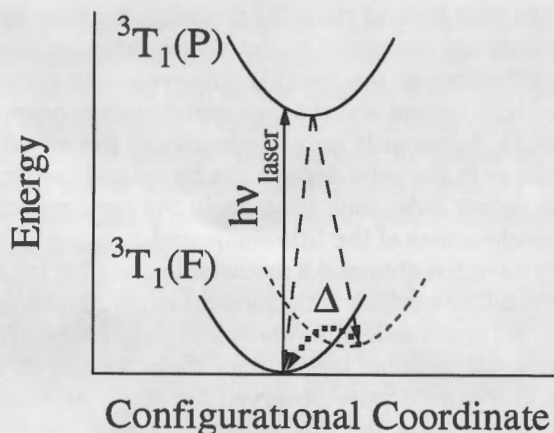


Figure 5. Schematic view of the spectroscopic transitions used for optical switching to the laser-induced metastable state for dibromobis(4-methylthiazole)nickel(II). The solid and dotted potential energy curves at low energy denote the blue and yellow forms of the title compound, respectively.

build up a significant population of the metastable state, whereas at higher temperatures thermally activated relaxation between the two low-energy states rapidly depopulates the metastable state. This relaxation process is indicated by the dotted arrow and the thermal activation barrier Δ in Figure 5.

Spectroscopic evidence for the presence of a metastable state is obtained from the difference absorption spectra in Figure 4. At 80 K, the integrated difference shown in the inset to Figure 4 becomes smaller with time and vanishes after approximately 30 min, a typical behavior indicating the presence of a long-lived metastable state (7). The temperature dependence of the integrated differences in Figure 4 shows that the lifetime of the metastable state at 30 K is much longer than an hour, whereas at 150 K it is shorter than 5 minutes. This temperature dependence is typical for a thermally activated relaxation of the metastable state and it confirms this first experimental observation of the inverse thermochromic transition for dibromobis(4-methylthiazole)nickel(II). The increase of the absorption in the blue spectral region, expected for the yellow form of the compound, is more difficult to follow than the decrease of the lower energy band. We note a negative difference spectrum between 20,000 cm⁻¹ and 25,000 cm⁻¹ for the trace recorded 5 min after laser irradiation, indicating an increase of the absorbance in this region. This difference also vanishes at long times, as illustrated by comparing the top and bottom difference spectra with their horizontal baselines. The integrated positive and negative differences are comparable in magnitude, but they are not expected to be equal because of the different transition moments for the two bands. We note

that the blue form of the solid deposit is far from being quantitatively converted to the yellow form, an important difference to the iron(II) spin-crossover systems, where both optical and thermal switching are quantitative (6,7). Apparently only a minority of the nickel(II) complexes in the solid deposit can be optically switched to the yellow form, indicating again the very particular thermochromism of the title compound.

We have not obtained a metastable state for the single crystalline samples with the same experimental technique. No systematic differences and no deviations from a horizontal baseline larger than those for the 60 min trace in Figure 4 were observed for single crystals. A likely explanation for this behavior is that the disordered structure of the solid deposit facilitates the formation of the metastable state. The changes of both structure and coordination between the blue and yellow forms of this compound are expected to be large, schematically illustrated by the very different position of the minima of the two low-energy potential curves along the configurational coordinate in Figure 5. These large changes prohibit the conversion between the two forms for molecules embedded in an ordered solid with close packing of chromophores, an aspect that has been discussed in detail for the spin-crossover transition of iron(II) compounds (7). The different behavior of single crystals and solid deposits under laser irradiation again confirms the presence of two different blue forms of the title compound.

We are currently studying a series of other thermochromic compounds of nickel(II) in order to achieve a quantitative laser-induced transition to the metastable state. Materials with metastable states that persist to high temperature are most interesting because they offer the possibility of rapidly tunable colors by optical switching at room temperature. Transition metal compounds with their rich variety of excited electronic states are excellent candidates for an extended study of these phenomena.

Acknowledgements

This work was made possible by research grants from NSERC (Canada), FCAR (Province of Quebec) and an exchange fellowship from CREPUQ (Région Rhône-Alpes, France) to L.L.G. We thank Dr Claude Daul (Université de Fribourg, Switzerland) for his crystal field program.

References

1. J. Ferguson, *Progr. Inorg. Chem.*, **12**, 159 (1970).
2. P. J. McCarthy and H. U. Güdel, *Coord. Chem. Rev.*, **88**, 69 (1988).
3. "Electronic and Vibronic Spectra of Transition Metal Complexes I", H. Yersin, Ed.; Topics in Current Chemistry, Vol. 171, Springer: Berlin, 1994.
4. J. I. Zink and K.-S. Kim Shin In *Adv. in Photochemistry*; D. H. Volman, G. S. Hammond and D. C. Neckers, Eds.; John Wiley: New York, 1991; Vol. 16; p. 119.
5. C. Reber and J. I. Zink, *Comments on Inorg. Chem.*, **13**, 177 (1992).
6. S. Decurtins, P. Güthlich, K. M. Hasselbach, A. Hauser and H. Spiering, *Inorg. Chem.*, **24**, 2174 (1985).
7. P. Güthlich, A. Hauser and H. Spiering, *Angewandte Chemie International Edition in English*, **33**, 2024 (1994) and references therein.
8. D.R. Bloomquist and R. D. Willett, *Coord. Chem. Rev.*, **47**, 125 (1982).
9. J. A. Weaver, P. Hambricht, P. T. Talbert, E. Kang and A. N. Thorpe, *Inorg. Chem.*, **9**, 268 (1970).
10. M. N. Hughes and K. J. Rutt, *Inorg. Chem.*, **10**, 414 (1971).
11. R. P. Kurkijy and E. V. Brown, *J. Am. Chem. Soc.*, **74**, 5778 (1952).
12. D. Wexler, J. I. Zink and C. Reber, *J. Phys. Chem.*, **96**, 8757 (1992).
13. A. B. P. Lever, *Inorg. Chem.*, **4**, 763 (1965).
14. C. J. Ballhausen, "Introduction to Ligand Field Theory"; McGraw-Hill, New York, 1962.
15. S. Sugano, Y. Tanabe and H. Kamimura, "Multiplets of Transition Metal Ions in Crystals"; Academic Press, New York, London, 1970.
16. E. König and S. Kremer, "Ligand Field Energy Diagrams". Plenum Press, New York and London, 1977.
17. C. Reber and H. U. Güdel, *Inorg. Chem.*, **25**, 1196 (1986).
18. C. J. Ballhausen, *Z. Phys. Chem.*, **17**, 246 (1958).